

All Figures in Two Articles by LIU Yueliang (刘月亮) Are Identical and Derived from a Single Master's Thesis

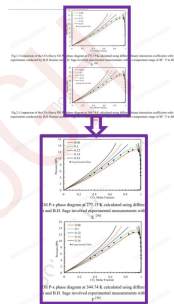
An investigation conducted by the 5GH Team has revealed that two articles, [1] and [2], contain 20 identical figures, all of which are reused from the Master's Thesis of LIU Wenbin, a former student at China University of Petroleum (East China).

Every figure in Article [1] matches the corresponding figure in Article [2] exactly. Furthermore, all 20 figures are directly reproduced from LIU Wenbin's Master's Thesis.

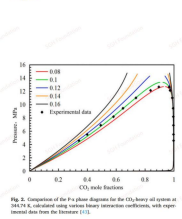
In addition to the reused figures across both articles, the investigation also identified that multiple passages in Article [1] were paraphrased from Article [2].

Examples of the reused figures and paraphrased passages are provided below:

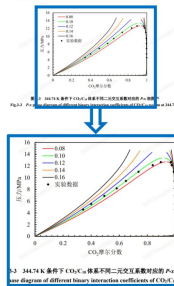
10.1016/j.cej.2026.173309
Fig 1, 2



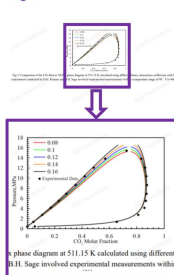
10.1016/j.energy.2025.137818
Fig 2



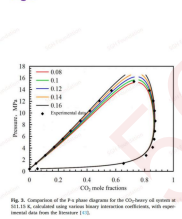
LIU Wenbin, Master Thesis
Fig 3-3



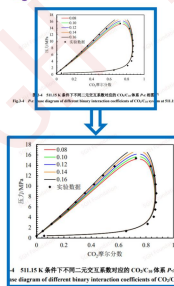
10.1016/j.cej.2026.173309
Fig 3



10.1016/j.energy.2025.137818
Fig 3



LIU Wenbin, Master Thesis
Fig 3-4



10.1016/j.cej.2026.173309
Fig 4, 5

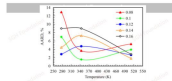


Fig. 4. Temperature dependence of ASEP and other binary interaction parameters for the CO₂-DME system.



Fig. 5. Procedure for the phase diagram of the CO₂-DME system.

10.1016/j.energy.2025.137818
Fig 3

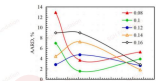


Fig. 4. Dependence of the vapor-liquid critical temperature (T_c) on the composition of the CO₂-DME system.

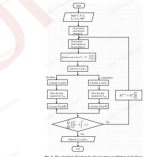


Fig. 5. Procedure for the phase diagram of the CO₂-DME system.

LIU Wenbin, Master Thesis
Fig 3-4, 3-1

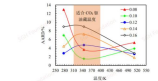


Fig. 4. Dependence of the vapor-liquid critical temperature (T_c) on the composition of the CO₂-DME system.



Fig. 5. Procedure for the phase diagram of the CO₂-DME system.

10.1016/j.cej.2026.173309
Fig 6, 7

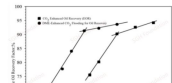


Fig. 6. Dependence of the vapor-liquid critical temperature (T_c) on the composition of the CO₂-DME system.

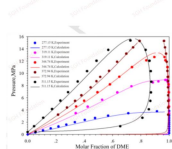


Fig. 7. P-T phase diagram for the CO₂-DME binary system. Solid data represent experimental data [11,12], while solid lines denote the predictions from the thermodynamic equation of state.

10.1016/j.energy.2025.137818
Fig 6, 7

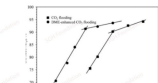


Fig. 6. Dependence of the vapor-liquid critical temperature (T_c) on the composition of the CO₂-DME system.

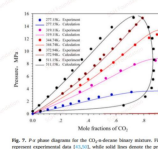


Fig. 7. P-T phase diagram for the CO₂-DME binary system. Solid data represent experimental data [11,12], while solid lines denote the predictions from the thermodynamic equation of state.

LIU Wenbin, Master Thesis
Fig 3-23, 3-10

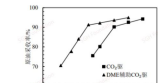


Fig. 6. Dependence of the vapor-liquid critical temperature (T_c) on the composition of the CO₂-DME system.

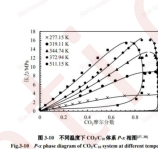


Fig. 10. P-T phase diagram of CO₂-DME system at different temperatures.

10.1016/j.cej.2026.173309
Fig 8, 9

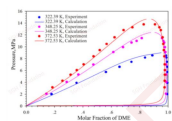


Fig. 8. P-T phase diagram for the CO₂-DME binary system. Solid data represent experimental data [11,12], while solid lines denote the predictions from the thermodynamic equation of state.

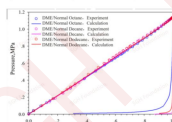


Fig. 9. P-T phase diagram for the CO₂-DME binary system. Solid data represent experimental data [11,12], while solid lines denote the predictions from the thermodynamic equation of state.

10.1016/j.energy.2025.137818
Fig 8, 9

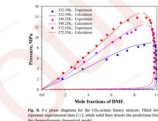


Fig. 8. P-T phase diagram for the CO₂-DME binary system. Solid data represent experimental data [11,12], while solid lines denote the predictions from the thermodynamic equation of state.

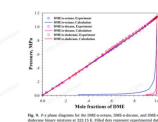


Fig. 9. P-T phase diagram for the CO₂-DME binary system. Solid data represent experimental data [11,12], while solid lines denote the predictions from the thermodynamic equation of state.

LIU Wenbin, Master Thesis
Fig 3-8, 3-14

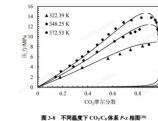


Fig. 8. P-T phase diagram for the CO₂-DME binary system. Solid data represent experimental data [11,12], while solid lines denote the predictions from the thermodynamic equation of state.

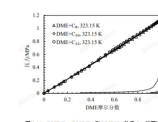


Fig. 14. P-T phase diagram of DME-CO₂ system at different temperatures.

10.1016/j.cej.2026.173309
Fig 10, 11

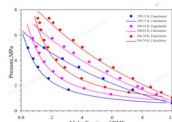


Fig. 10. P-T phase diagram for the CO₂-DME binary system. Solid data represent experimental data [11,12], while solid lines denote the predictions from the thermodynamic equation of state.

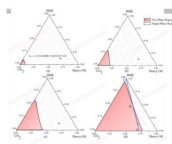


Fig. 11. Ternary phase diagram for the CO₂-DME binary system. Solid data represent experimental data [11,12], while solid lines denote the predictions from the thermodynamic equation of state.

10.1016/j.energy.2025.137818
Fig 10, 11

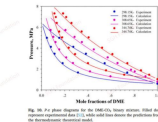


Fig. 10. P-T phase diagram for the CO₂-DME binary system. Solid data represent experimental data [11,12], while solid lines denote the predictions from the thermodynamic equation of state.

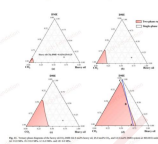


Fig. 11. Ternary phase diagram for the CO₂-DME binary system. Solid data represent experimental data [11,12], while solid lines denote the predictions from the thermodynamic equation of state.

LIU Wenbin, Master Thesis
Fig 3-15, ---

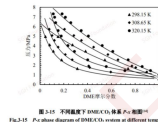


Fig. 15. P-T phase diagram for the CO₂-DME binary system. Solid data represent experimental data [11,12], while solid lines denote the predictions from the thermodynamic equation of state.

10.1016/j.cej.2026.173309
Fig 12, 13

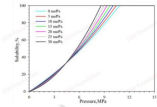


Fig. 12. CO₂ solubility in binary and within the binary and CO₂-DME system

10.1016/j.energy.2025.137818
Fig 12, 13

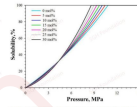


Fig. 13. Solubility of CO₂ in binary and within the binary and CO₂-DME system with different mole fraction of DME

LIU Wenbin, Master Thesis
Fig ---, ---

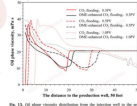
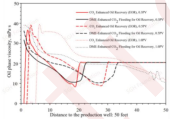
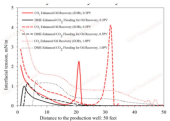
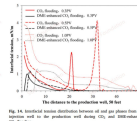


Fig. 15. CO₂ phase density distribution from the formation well to the production well using the different CO₂-DME systems

10.1016/j.cej.2026.173309
Fig 14, 15



10.1016/j.energy.2025.137818
Fig 14, 15



LIU Wenbin, Master Thesis
Fig 3-24, 3-28

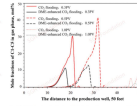
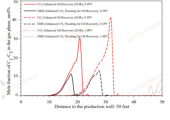


Fig. 16. CO₂ phase density distribution from the formation well to the production well for the production well using CO₂ and DME relative CO₂-DME systems

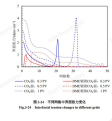
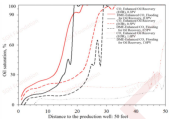


Fig. 17. CO₂ phase density distribution from the formation well to the production well for the production well using CO₂ and DME relative CO₂-DME systems

10.1016/j.cej.2026.173309
Fig 16, 17



10.1016/j.energy.2025.137818
Fig 16, 17

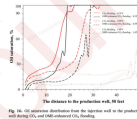


Fig. 18. CO₂ phase density distribution from the formation well to the production well using CO₂ and DME relative CO₂-DME systems

LIU Wenbin, Master Thesis
Fig 3-25, 3-32

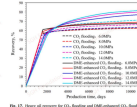
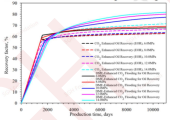


Fig. 19. CO₂ phase density distribution from the formation well to the production well using CO₂ and DME relative CO₂-DME systems

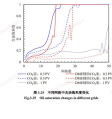
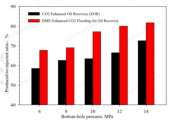


Fig. 20. CO₂ phase density distribution from the formation well to the production well using CO₂ and DME relative CO₂-DME systems

10.1016/j.cej.2026.173309
Fig 18, 19



10.1016/j.energy.2025.137818
Fig 18, 19

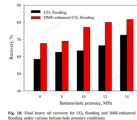


Fig. 21. CO₂ phase density distribution from the formation well to the production well using CO₂ and DME relative CO₂-DME systems

LIU Wenbin, Master Thesis
Fig ---, 3-35

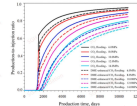
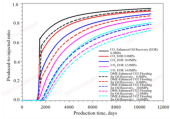


Fig. 22. CO₂ phase density distribution from the formation well to the production well using CO₂ and DME relative CO₂-DME systems

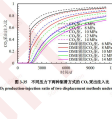


Fig. 23. CO₂ phase density distribution from the formation well to the production well using CO₂ and DME relative CO₂-DME systems

